Desalination and Water Treatment
www.deswater.com

doi: 10.5004/dwt.2019.24190

158 (2019) 164–173
August

Adsorption of Cu(II) and Pb(II) from aqueous solutions onto a metakaolin-based geopolymer

Peifei Ding, Weifeng Song*, Chao Wang, Zefeng Yu

School of Environmental Science and Engineering, Guangdong University of Technology, Guangzhou, 510006, China, Tel. +86 39322037; email: weifengsong@gdut.edu.cn (W. Song)

Received 20 November 2018; Accepted 27 March 2019

ABSTRACT

Metakaolin-based geopolymer was investigated as absorbent to remove Cu(II) and Pb(II) from aqueous solution. The effects of adsorbent quantity, pH, contact time, and initial concentration of Cu(II)/Pb(II) in solutions were investigated. Furthermore, kinetics and isothermal adsorption were fitted by using equations. Kinetic adsorption of Cu(II) and Pb(II) fitted well to pseudo-second-order model. The isothermal adsorption of two heavy metals by the metakaolin-based geopolymer fitted well with Langmuir isotherm adsorption model. The maximum monolayer adsorption capacities were found to be 178.6 mg/g (2.79 mmol/g) and 312.5 mg/g (1.51 mmol/g) for Cu(II) and Pb(II), respectively. Results clearly showed that the adsorption of metal ions on geopolymer was accompanied by ion exchange. Low-cost, convenient, and effective adsorption of Cu(II) and Pb(II) make metakaolin-based geopolymers potential candidates for heavy metal removal in wastewater treatment.

Keywords: Geopolymer; Copper; Lead; Removal; Adsorption

1. Introduction

Heavy metal pollution in the environment has attracted growing attention in recent years. Various sources, such as lead smelter, battery manufacture, boat and ship fuel, as well as ammunition industry produce and discharge wastewater containing different heavy metals into the environment. Owing to their toxic effects on the human body, heavy metals can pose a serious risk to human health [1]. Thus, safe and cost-effective removal of heavy metals from wastewater is extremely important. Conventional wastewater treatment processes include chemical precipitation [2], electrochemical treatment [3], adsorption [4], ion exchange [5,6], and membrane separation [7]. Among these methods, adsorption has the advantages of extensive sources, small secondary pollution, and low running cost and chemical inputs. At this stage, researchers are mainly looking for more reasonable, low-cost, high-quality adsorption materials, such as agricultural and forestry waste materials, industrial waste, zeolites [8] and biosorbents [9].

Geopolymers are ceramic-like inorganic polymers produced at low temperature, generally below 100°C, which consist of chains or networks of mineral molecules linked with covalent bonds [10]. In recent years, many studies have reported geopolymers as efficient heavy metal adsorbents. Duan et al. [11] examined fly ash and iron ore tailing-based porous geopolymers for the removal of Cu(II) from wastewater, and the adsorption capacity of the synthesized geopolymer reached 113.41 mg/g. Kara et al. [12] studied the adsorption of Zn(II) and Ni(II) on a metakaolin-based geopolymer adsorbent. The maximum adsorption monolayer capacities were found to be 1.14 and 0.726 mmol/g for Zn(II) and Ni(II), respectively. Both studies confirmed that geopolymers have good adsorption capacity for heavy metal ions present in wastewater and high adsorption activity as well. Geopolymers prepared using industrial waste fly ash or

---

* Corresponding author.

inorganic clay are more environmentally friendly and stable than organic adsorbents. They are low-cost materials with good chemical stability and abundant resources.

In the present study, metakaolin-based geopolymer was used as an effective adsorbent for the removal of Cu(II) and Pb(II) from aqueous solutions. The optimization of adsorption conditions including amount of adsorbent, pH, contact time, and initial concentrations of metal ions was systematically investigated. Furthermore, the kinetics of adsorption and the characteristics of the geopolymer were evaluated by Fourier transform infrared spectroscopy, X-ray diffraction, scanning electron microscopy energy-dispersive X-ray spectroscopy (SEM–EDS), and Brunauer–Emmett–Teller (BET) as well as pore size distribution analysis.

2. Materials and methods

2.1. Sample preparation

Kaolin was purchased from Aladdin Company (Shanghai, China) and calcined at 900°C for 1 h to produce metakaolin and then sieved through a 110 μm mesh. The chemical composition of the metakaolin is as follows: 56.73% SiO_2, 37.26% Al_2O_3, 2.79% SO_3, 1.27% TiO_2, 0.92% Fe_2O_3, 0.76% CaO, and 0.17% K_2O. An activating alkali solution was prepared by mixing NaOH, Na_2SiO_3, and $NaAlO_2$ (analytical grade) in a molar ratio of 1:2.78:1.25. The metakaolin powder was then added into the prepared activating solution with a solid-to-liquid ratio of 1.5 g/50 mL, and then samples were dried at 60°C for 24 h. A flow-chart of the preparation process is shown in Fig. 1. Cu(II) and Pb(II) ions solutions were obtained by dissolving $Cu(NO_3)_2\cdot 3H_2O$ (analytical grade) and $Pb(NO_3)_2$ (analytical grade) in distilled water.

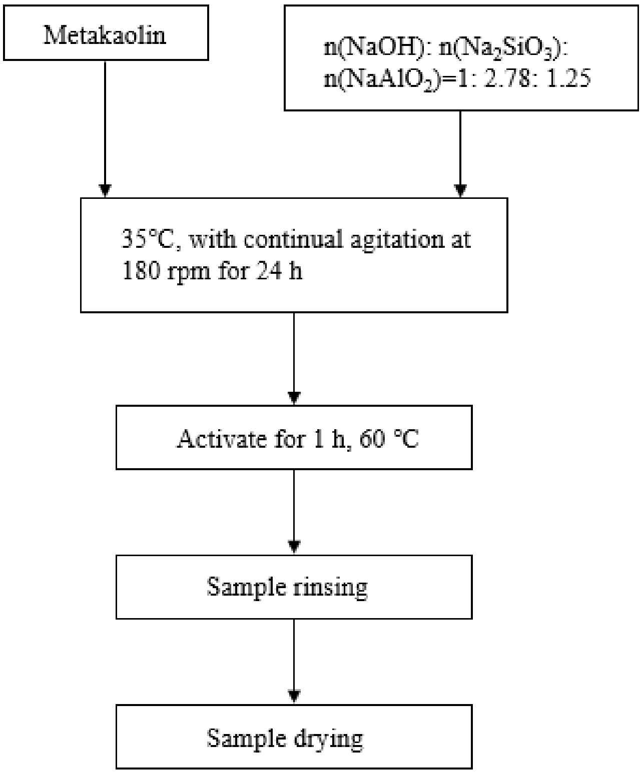

Fig. 1. Flow-chart of the preparation process of the geopolymer.

2.2. Characterization

To investigate whether ion exchange occurs during the adsorption process, EDS spectra of the geopolymer were analyzed before and after metal adsorption by SEM (SU8220, Hitachi Company, Japan) operating at 20 kV. Samples were coated with a gold layer under vacuum prior to their analysis to increase their electrical conductivity. FTIR spectra (Nicolet 6700, Thermo Fisher Scientific, Waltham, MA, USA) of the geopolymer were measured before and after metal adsorption for microstructure evaluation. The mineral identification and crystallinity of the metakaolin and the geopolymer were characterized by XRD and recorded in the 2θ range of 10° to 70° with a scanning speed of 0.5°/min. Specific surface area and pore size distribution were determined via nitrogen sorption using a Micrometrics (Ottawa Ontario, Canada) ASAP 2020 BET analyzer. The geopolymer was previously degassed under vacuum, heated to 250°C for 6 h, and maintained at a pressure below 30 μm Hg for 15 min. The porous structures were obtained from the Barrett–Joyner–Halenda (BJH) data. The concentrations of Pb and Cu in the test solutions were measured by atomic adsorption spectrometry (AAS, HITACHI Z2000, Hitachi Limited, Tokyo, Japan).

2.3. Batch adsorption experiments

Adsorption experiments were performed in a rotary shaker (180 rpm), for the contact time of 0–300 min, by varying different parameters: adsorbent dose (0.1–1.4 g/L), pH (2–6) and initial metal concentrations (100–600 mg/L), in order to optimize the reaction conditions. The pH value of the solution was adjusted with 0.1 M HCl and 0.1 M NaOH. After shaking the flasks, the supernatant was filtered through a 0.22 μm cellulose nitrate filter for Cu(II) and Pb(II) analysis by AAS. Each adsorption experiment in this study was repeated at least three times.

The removal efficiency (R) of the metal ions at each interval of time is given by:

$$R(\%) = \frac{C_0 - C_e}{C_0} \times 100 \tag{1}$$

The adsorption capacity (Q_e) is calculated by using the following equation:

$$Q_e = \frac{C_0 - C_e}{m} \times V \tag{2}$$

where Q_e (mg/g) is the adsorption capacity of the adsorbent, C_0 and C_e (mg/L) are the initial and equilibrium concentrations of the metal ions, respectively, and M is the mass of the adsorbent (g) taken in V (L) volume of solution.

3. Results and discussion

3.1. Characterization of the geopolymer

Fig. 2 shows the XRD patterns of metakaolin and the metakaolin-based geopolymer. Results show that the kaolinite peak decreases with the formation of the geopolymer [13], and that the geopolymer is an amorphous material, due to the presence of a very broad peak in Fig. 2b. The peak observed at 2θ = 26° corresponds to unreacted quartz, which has been reported in literature study [14–16].

Types of functional groups present on the adsorbent surface were examined using FTIR spectra before and after adsorption of Cu(II)/Pb(II) ions and are presented in Fig. 3. The absorption band at 3,426 cm^{-1} is attributed to the presence of –OH bond, while the peak at 1,023 cm^{-1} corresponds to the presence of Si–O–Si (Al) asymmetric stretch band [17]. The absorption band of H–O–H bending vibration at 1,636 cm^{-1} in the IR spectrum of the unloaded adsorbent was observed at 1,642 cm^{-1} after Cu(II) and Pb(II) adsorption. The bands appearing at 682 cm^{-1} are attributed to Al–O–Si vibrations, and the peak at 518 cm^{-1} corresponds to the presence of Si–O–Al in an octahedral coordination [18]. The peak at 1,511 cm^{-1} clearly shifts to 1,488 cm^{-1} after Cu(II) adsorption, which indicates the formation of the chemical bonds between the heavy metal ions and the geopolymer [19]. The band at 1,400 cm^{-1} in the spectra of Pb(II)-loaded geopolymer corresponds to the asymmetric stretching vibration of the O–C–O bonds of CO_3^{2-}, which appears probably due to atmospheric carbonation on the surface of the geopolymer [17,20]. The results showed that the structure of the geopolymer has not changed distinctly after the adsorption of Cu(II) and Pb(II).

The geopolymer samples before and after adsorption of Cu(II) and Pb(II) were analyzed by SEM and results are shown in Fig. 4. Fig. 4a exhibits that the surface of the geopolymer is a loose structure, attributed to the formation a gel structure network due to the alkaline activation [21]. The microstructure of the samples did not show any significant changes after adsorption, but became more compact [22]. Fig. 4b shows the EDS results, indicating that the main elements present in the geopolymer are Si, Al, Na, which is consistent with the reactants used for the preparation of the geopolymer. After Cu(II) and Pb(II) adsorption, the Na peak decreases and Cu/Pb peaks become visible in the spectra, which may be due to the replacement of Na^+ ions by Cu^{2+} or Pb^{2+} ions in the adsorption process by ion exchange, as presented in Figs. 4b(II) and (III).

The porous structure of the material plays an important role in the removal of heavy metals from wastewater. Therefore, the specific surface area (S_{BET}), and the micropores of the geopolymer and metakaolin were measured (Fig. 5). The S_{BET} of the geopolymer increased from 3.2 m^2/g for the metakaolin to 32 m^2/g, because of the significant improvement in the adsorption effect. According to the classification of the International Union of Pure and Applied Chemistry (IUPAC), the corresponding isotherm for the adsorbent (Fig. 5a) corresponds to a type IV isotherm with a distinct H3 hysteresis loop, which is characteristic of mesoporous materials [23]. Fig. 5b shows that the pore size distribution of the geopolymer is in the range of 0.87–28.9 nm, with the most probable pore radius of 3.05 nm, which proves that the geopolymer is mesoporous (2–50 nm). The most probable pore radius of the geopolymer after adsorption of Cu(II) and Pb(II) decreased to 3.02 nm, indicating that the adsorbed heavy

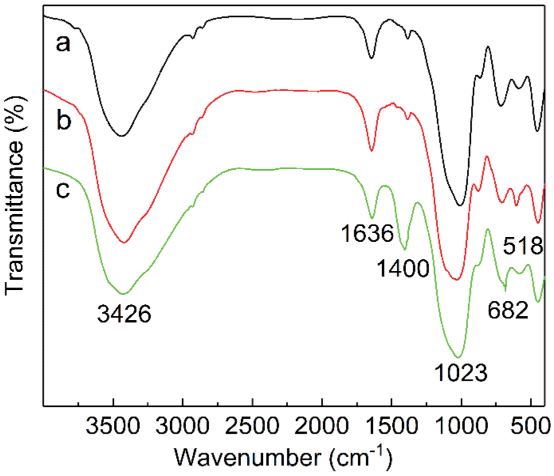

Fig. 3. FTIR spectra of the (a) geopolymer, (b) Cu(II)-loaded geopolymer, and (c) Pb(II)-loaded geopolymer.

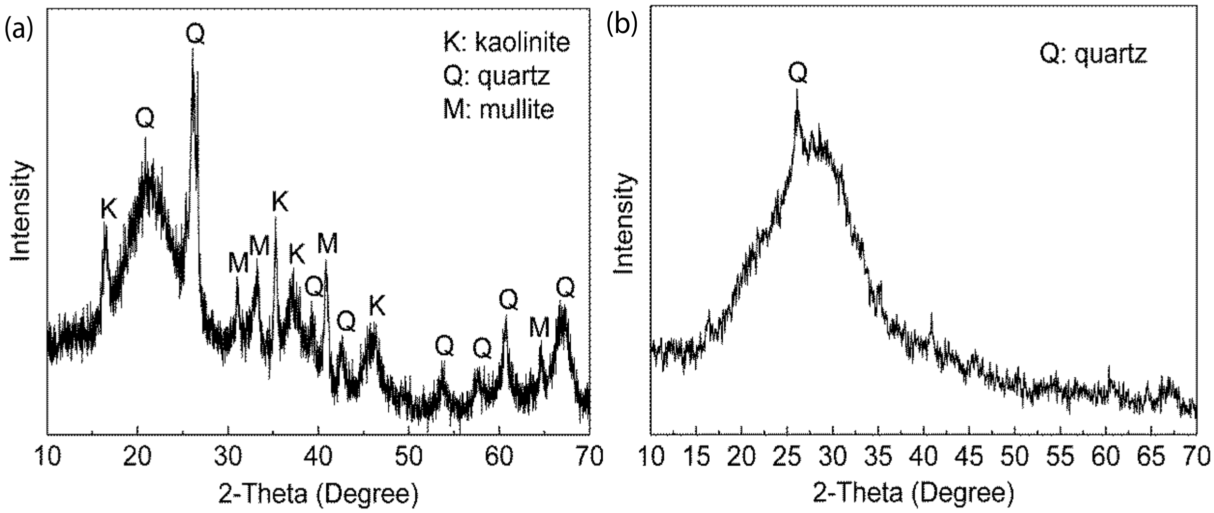

Fig. 2. XRD patterns of (a) metakaolin and (b) geopolymer.

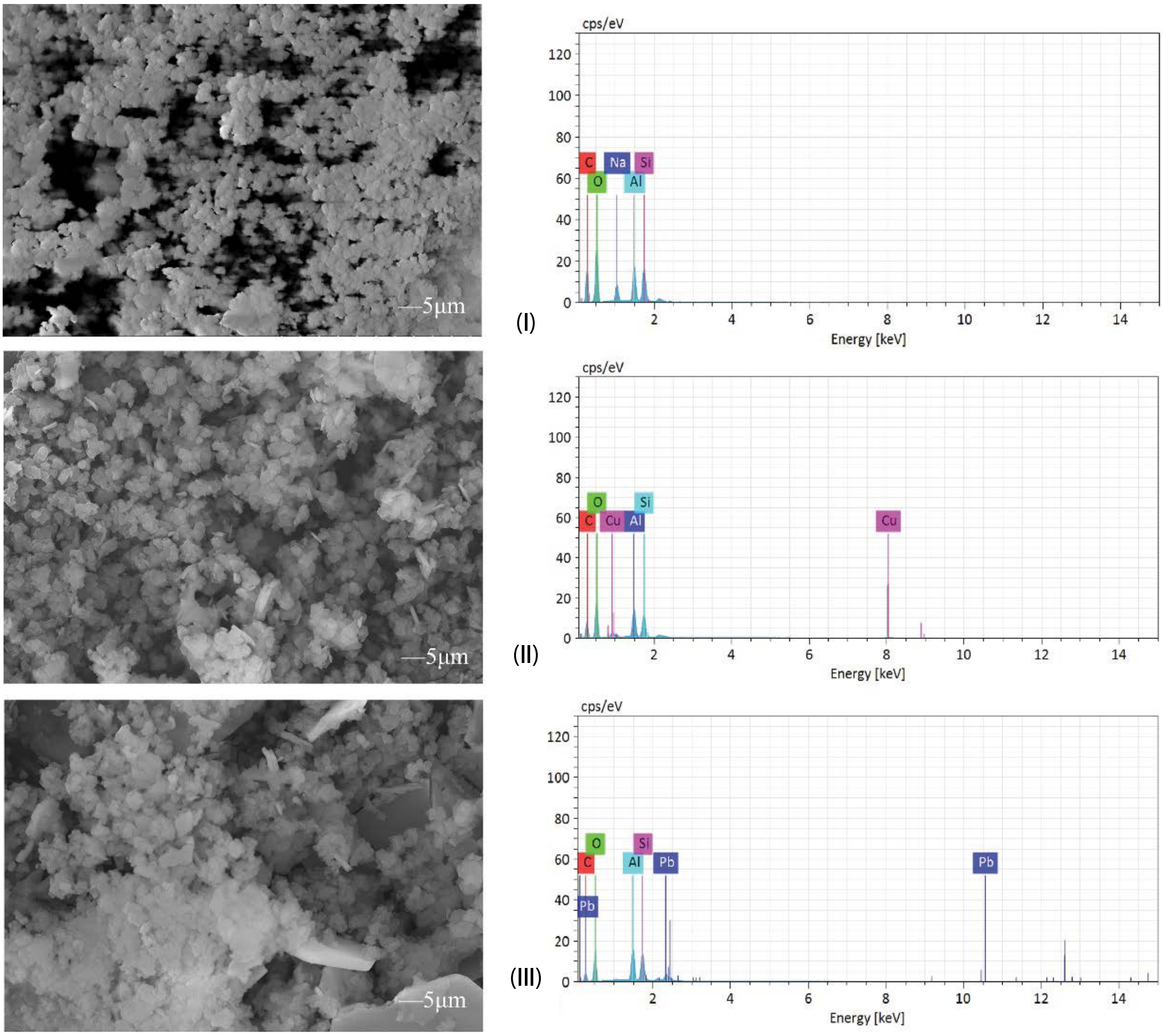

(a) (b)

Fig. 4. (a) SEM image and (b) EDS spectra of the (I) geopolymer, (II) Cu(II)-loaded geopolymer, and (III) Pb(II)-loaded geopolymer.

metal ions slightly affected the mesoporous structure of the geopolymer. The values of S_{BET} of Cu(II)-loaded geopolymer and Pb(II)-loaded geopolymer are 22.85 and 24.9 m^2/g, respectively.

3.2. Effect of the geopolymer dosage on the sorption of Cu(II) and Pb(II)

Fig. 6 shows the sorption efficiency for Cu(II) and Pb(II) as a function of the geopolymer dosage. With the increase in the geopolymer amount from 0.2 to 0.8 g/L, the removal efficiency of Cu(II) increases by 47%. In contrast, the removal efficiency of the Pb(II) increases rapidly by 30% with the increase in the geopolymer dosage from 0.1 to 0.3 g/L. It could be assumed that when the dosage of the geopolymer increased, the number of active sites available for sorption also increased. Further increase in the geopolymer dosage did not result in any significant increase in the adsorption of Pb(II), and it reached a constant when the geopolymer dosage was 0.3 g/L. However, when the geopolymer dosage increased, the adsorption capacities (q) decreased. This was attributed to the fact that the initial concentration of metal ions in the solution did not change, resulting in an excess of active sites, and the adsorption amount was gradually reduced. Consequently, the optimum dosage of the geopolymer was found to be 0.6 g/L for Cu(II), and 0.3 g/L for Pb(II).

3.3. Effect of pH

The effect of pH of the solution on the adsorption of Cu(II) and Pb(II) by the geopolymer was investigated in the

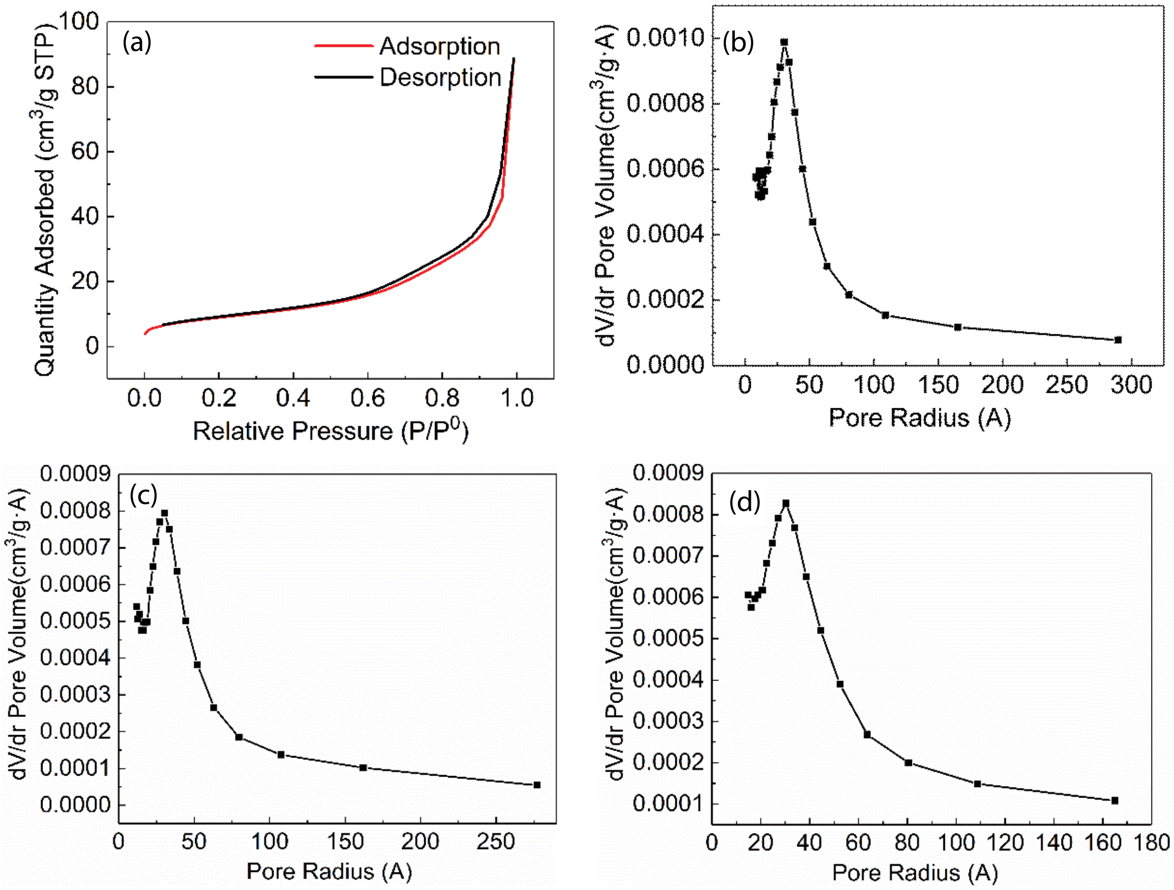

Fig. 5. (a) N_2 adsorption–desorption isotherm of the geopolymer; and BJH pore-size distribution of the (b) geopolymer, (c) Cu(II)-loaded geopolymer, and (d) Pb(II)-loaded geopolymer.

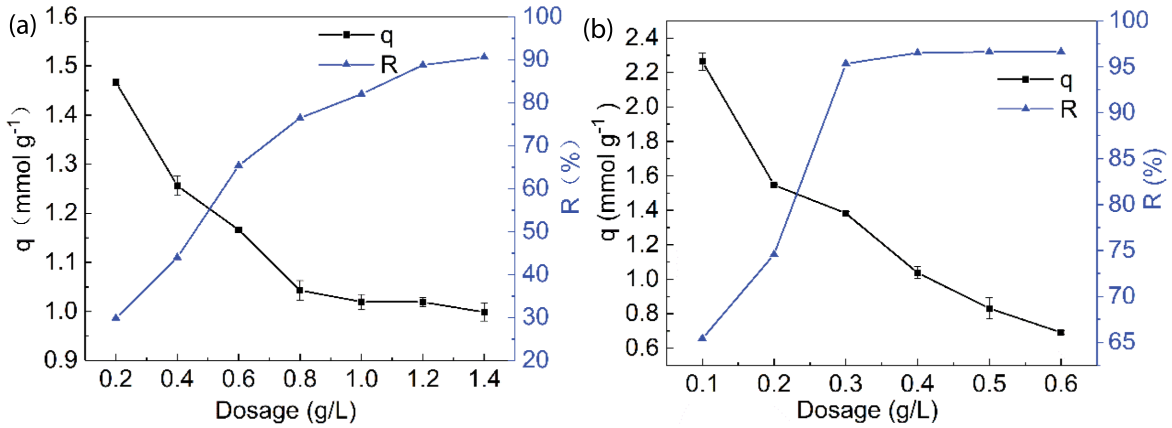

Fig. 6. Effect of the geopolymer dosage on the metal sorption of (a) Cu(II) and (b) Pb(II). The initial concentration of Cu(II) and Pb(II) was 100 mg/L; pH: 5.0; temperature: 30°C; reaction time: 3h.

pH range from 2 to 6, as shown in Fig. 7. The pH of the aqueous solution is an important factor in the adsorption process because it affects the surface charge of the adsorbents, the solubility of the metal ions, and the degree of ionization and speciation of the adsorbate during reactions [24]. Fig. 7 demonstrates that the adsorbent shows an increase in the adsorption of both Cu(II) and Pb(II) with the increase in the pH of both metal ion solutions. At low pH, metal ions and H^+ ions could compete for binding sites on the geopolymer, and the active surface sites of the adsorbent could be easily occupied by H^+ ions, thus reducing the adsorption of metal ions. With the increase in pH, the H^+ ions concentration decreases and the competition becomes weaker, thus the adsorption capacity for metal ions becomes stronger. High pH causes Cu(II) and Pb(II) to precipitate, thus pH 5 was selected as optimum value in both cases for further adsorption experiments.

3.4. Adsorption kinetics

Fig. 8a shows the effect of contact time on the sorption of Cu(II) and Pb(II) by the adsorbent. In these experiments, the initial concentration of Cu(II) and Pb(II) was 100 mg/L, respectively, the pH was set at 5, and the temperature was 30°C. The absorbed amount of Cu(II) and Pb(II) increased with increasing contact time, and reached equilibrium after 3.5 h for both Cu(II) and Pb(II). Based on these results, a contact time of 3.5 h was selected for subsequent sorption experiments.

Pseudo-first-order kinetic and pseudo-second-order kinetic models are commonly used to determine the factors that control the reaction rates and to observe the mechanism of metal adsorption by the geopolymer. They are given by Eqs. (3) and (4) [25] as follows:

$$\log\left(q_e - q_t\right) = \log q_e - \frac{\left(k_1\right)t}{2.303} \tag{3}$$

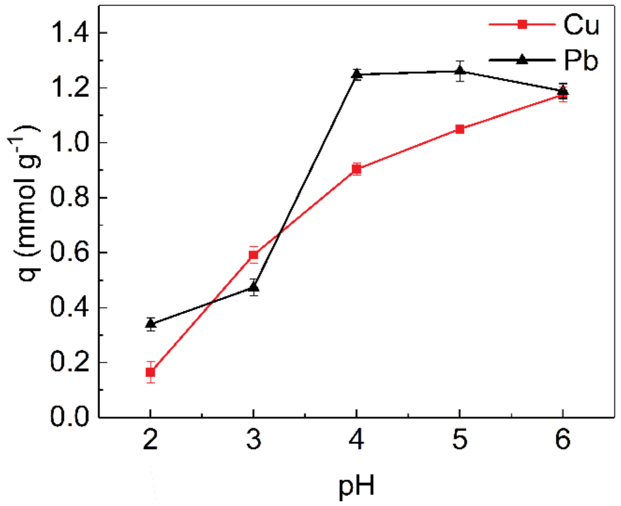

Fig. 7. Effect of pH on the adsorption of Cu(II) and Pb(II) by the adsorbent. The initial concentration of Cu(II) and Pb(II) was 100 mg/L; the dose of adsorption of Cu(II) was 0.6 g/L and the dose of adsorption of Pb(II) was 0.3 g/L; temperature: 30°C; reaction time: 3 h.

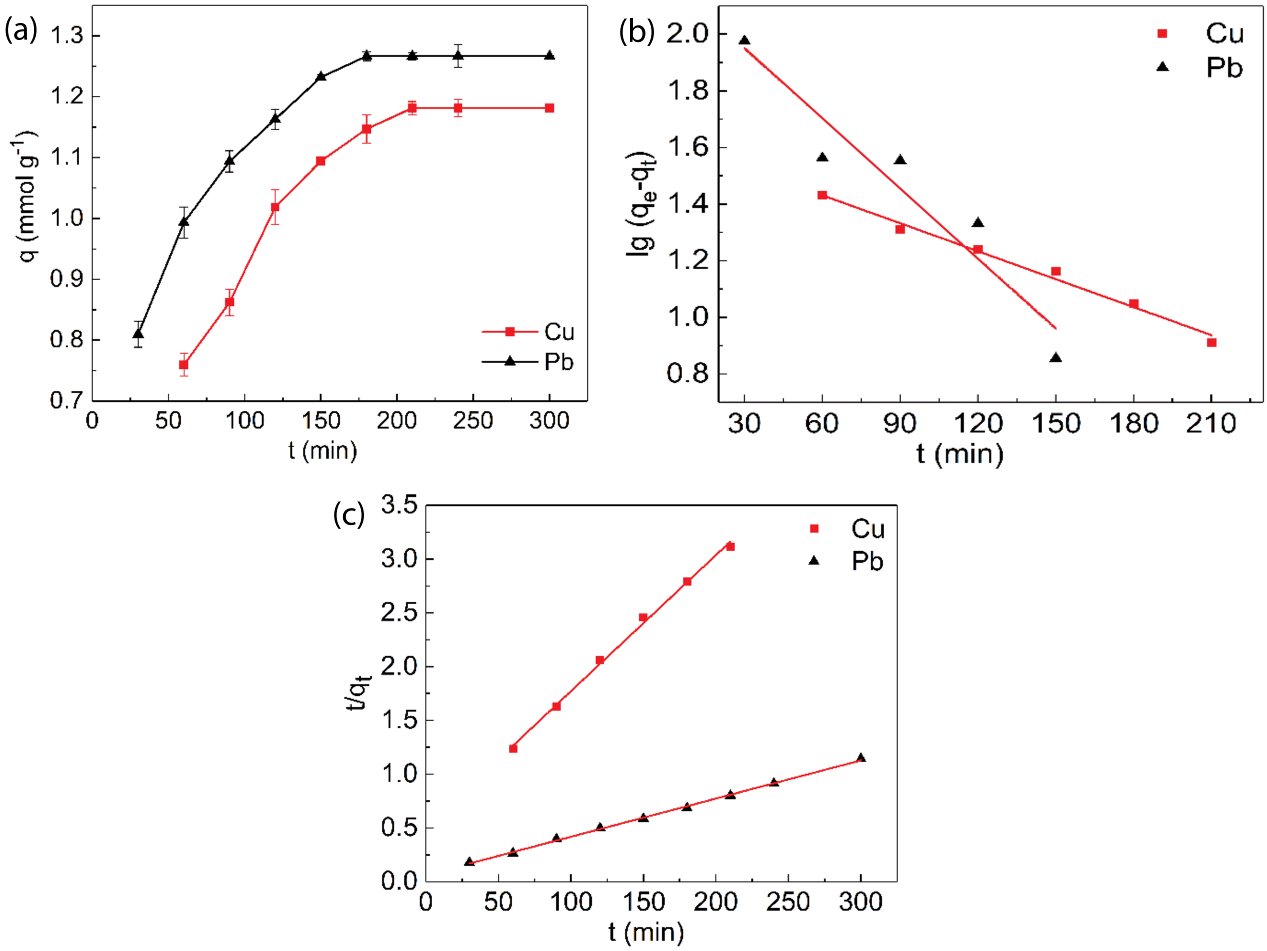

Fig. 8. (a) Effect of contact time on metal sorption of Cu(II) and Pb(II), (b) pseudo-first-order plots for adsorption of Cu(II) and Pb(II) by the geopolymer, and (c) pseudo-second-order plots for adsorption of Cu(II) and Pb(II) by the geopolymer.

$$\frac{t}{q_t} = \frac{1}{k_2 q_e^2} + \frac{t}{q_e} \tag{4}$$

where q_e and q_t (mg/g) represent the amounts of metal adsorbed at equilibrium time and at any time t (min), respectively; k_1 (min^{-1}) is the first-order rate constant; and k_2 (g mg^{-1} min^{-1}) is the second-order rate constant. Figs. 8b and c and Table 1 indicate that the kinetics of Cu(II) and Pb(II) ions sorption onto the geopolymer follows the pseudo-second-order model with an R^2 value of 0.997 and 0.999, respectively. Furthermore, the theoretical q_e values of the pseudo-second-order kinetic model were much closer to the experimental values. The calculated q_e values obtained were 78.74 mg/g for Cu(II) and 277.8 mg/g for Pb(II), while the experimental q_e values were 75.61 mg/g for Cu(II) and 262.2 mg/g for Pb(II). Therefore, the adsorptions of Cu(II) and Pb(II) ions were well fitted by pseudo-second-order kinetic, indicating the chemisorption between geopolymer and metal ions [26].

Table 1
Calculated kinetic parameters for adsorption of Cu(II) and Pb(II) by the geopolymer

Metal ion	Pseudo-first-order kinetic model			Pseudo-second-order kinetic model		
	q_e	k_1 (×10^{-4})	R^2	q_e	k_2 (×10^{-4})	R^2
Cu(II)	42.55	76.00	0.988	78.74	1.613	0.997
Pb(II)	157.7	188.9	0.916	277.8	2.031	0.999

3.5. Adsorption isotherms

The initial concentrations of Cu(II) and Pb(II) were adjusted in the range of 100–600 mg/L with pH 5 at 30°C for 3.5 h (Fig. 9a). The increase in the metal ions concentration resulted in an improvement in the removal of Cu(II) and Pb(II) by the geopolymer. This may be due to the further utilization of active sites of the geopolymer with the increase in the concentration of metal ions.

The adsorption capacity of the adsorbent mainly depends on the equilibrium concentration of the metal adsorbates in solution, and the correlation between them

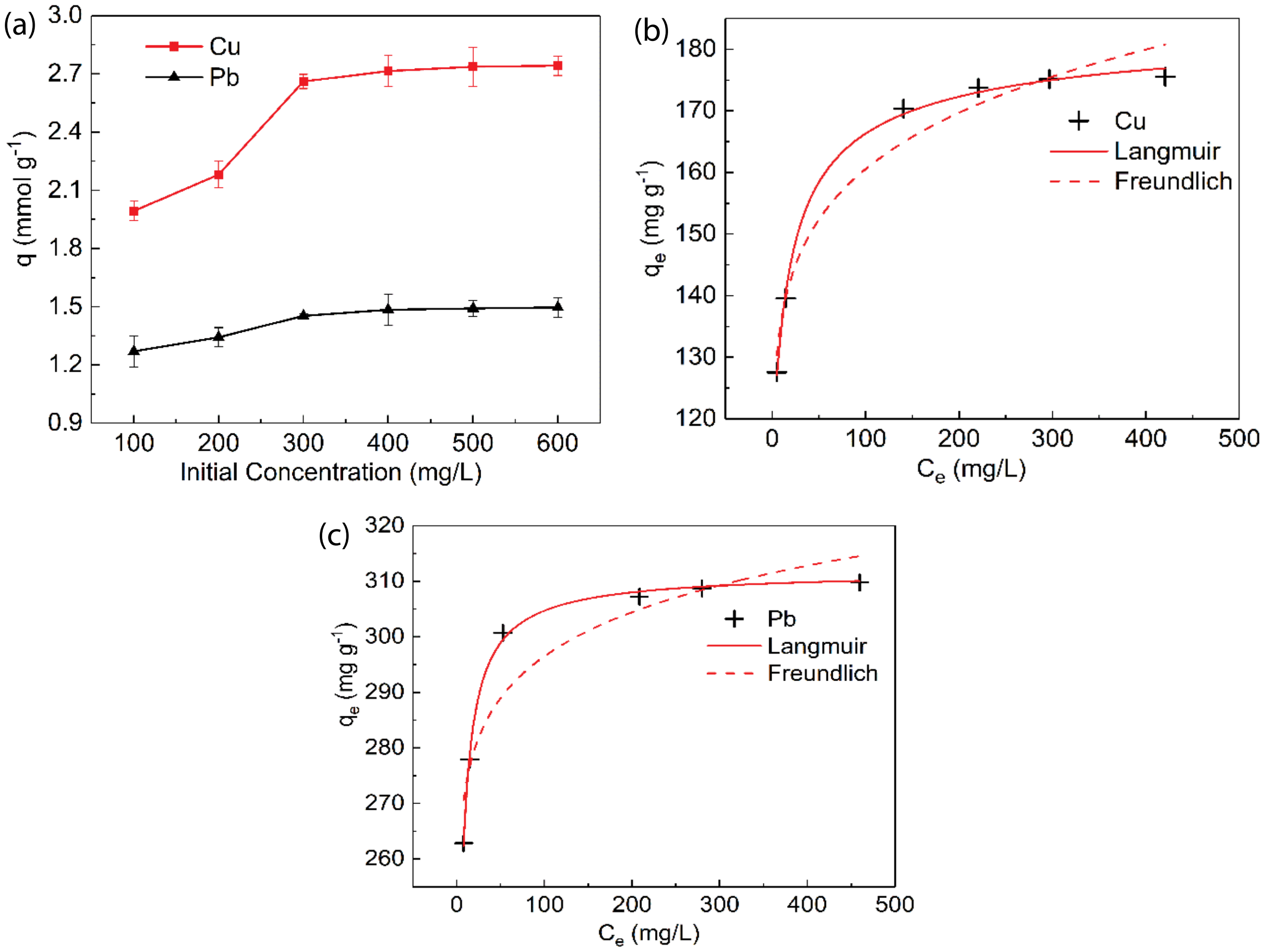

Fig. 9. (a) Effect of the initial concentration on the metal sorption of Cu(II) and Pb(II) by geopolymer, (b) adsorption isotherm of Cu(II), and (c) Pb(II) fitted by Langmuir and Freundlich models.

is described in terms of the adsorption isotherms at a given temperature. In this study, three isotherm models, namely, Langmuir [27], Freundlich, and Redlich–Peterson, were used to fit the equilibrium data for the adsorption of Cu(II) and Pb(II) ions onto the geopolymer.

The basic assumptions of Langmuir isotherm are as follows: (a) monomolecular layer adsorption; (b) the surface is homogeneous; and (c) the adsorption at one site does not affect the adjacent site. To determine the maximum adsorption capacity from aqueous single metal solutions, the following equation was employed:

$$\frac{C_e}{q_e} = \frac{1}{q_m^b} + \frac{C_e}{q_m} \tag{5}$$

where C_e (mg/L) is the equilibrium concentration, q_e (mg/g) is the amount adsorbed per unit mass of adsorbent at equilibrium, while q_m and b are the Langmuir constants related to the adsorption capacity and energy of adsorption, respectively.

The favorability of the adsorption of Cu(II) and Pb(II) ions by the geopolymer can be described by an essential dimensionless factor R_L:

$$R_L = \frac{1}{1 + bC_0} \tag{6}$$

where C_0 is the initial concentration of Cu(II) or Pb(II) ions. The R_L value indicates the shape of the isotherm to be either unfavorable ($R_L > 1$), linear ($R_L = 1$), favorable ($0 < R_L < 1$), or irreversible ($R_L = 0$).

The Freundlich model is an empirical equation which considers the heterogeneity of the adsorbent surface:

$$\ln q_e = \ln K_f + \frac{1}{n}\ln C_e \tag{7}$$

Freundlich constants K_f and n relate to the adsorption capacity and intensity, respectively.

The Redlich–Peterson (R–P) isotherm model is applicable in both homogeneous as well as heterogeneous systems as it is an improvement over the Langmuir and Freundlich models [28]. R–P equation is given as Eq. (8):

$$q_e = \frac{K_R C_e}{1 + a_R C_e^{\beta}} \tag{8}$$

where K_R (L/g) is the R–P isotherm constant, a_R (mg^{-1}) is R–P isotherm constant, and β is the exponent ($0 < \beta < 1$).

The adsorption isotherms of Cu(II) and Pb(II) fitted by the Langmuir and Freundlich models are shown in Figs. 9b and c. The correlation coefficients and isotherm parameters presented in Table 2 indicate that the Langmuir isotherm fits better than the Freundlich and R–P models. The maximum

Table 2
Isotherm model constants and correlation for adsorption of Cu(II) and Pb(II) ions from aqueous solution

Metal	Langmuir				Freundlich			R–P			
	q_m (mmol/g)	b (mg^{-1})	R_L	R^2	K_f	N	R^2	K_R (L/g)	a_R (mg^{-1})	β	R^2
Cu	2.79	0.058	0.028	0.993	109.1	14.12	0.831	2	0.088	0.952	0.977
Pb	1.51	0.088	0.019	0.997	236.5	26.46	0.787	2	0.039	0.901	0.927

Table 3
Adsorption results of Cu(II) and Pb(II) onto different adsorbents from literature reports

Reference	Adsorbent material	Maximum adsorption capacity (mg/g)		Maximum adsorption capacity (mmol/g)	
		Cu	Pb	Cu	Pb
Jiang et al. [29]	Modified kaolin	–	32.2	–	0.156
He et al. [30]	β-Cyclodextrin polymers	164.4	196.4	2.57	0.949
Andrejkovičová et al. [31]	Metakaolin-based geopolymers	44.73	261.2	0.70	1.26
Khalid et al. [32]	Geopolymer-supported zeolites	–	37.9	–	0.183
Liu et al. [33]	A novel hybrid chelating material	317.8	586.7	4.97	2.83
Xu et al. [34]	Black wattle tannin-immobilized nanocellulose	51.85	53.37	0.81	0.258
Khaleque [35]	Large-pore diameter nano-adsorbent	–	169.34	–	0.818
Ghasemi et al. [36]	Developed Fig sawdust activated carbon	–	80.65	–	0.390
Awual et al. [37]	Nano-composite adsorbent	173.6	–	2.71	–
Naushad et al. [38]	Sodium dodecyl sulfate-Th(IV) tungstate	181.8	–	2.84	–
Naushad et al. [39]	Ti(IV) iodovanadate cation exchanger	–	18.8	–	0.09
This study	Metakaolin-based geopolymers	178.6	312.5	2.79	1.51

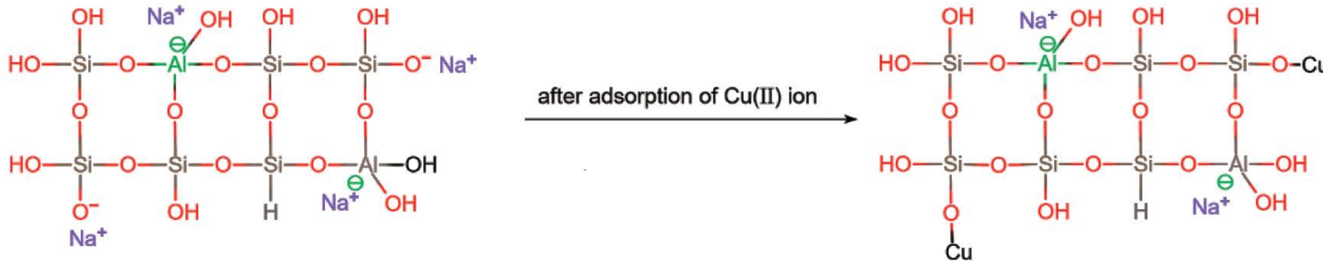

Fig. 10. Schematic illustration of adsorption mechanism.

adsorption capacity of Cu(II) and Pb(II) ions is 178.6 mg/g (2.79 mmol/g) and 312.5 mg/g (1.51 mmol/g), respectively. The results show that the adsorption of Cu(II) and Pb(II) ions by the geopolymer occurs as a monolayer adsorption, which may be due to the uniform and negligible interaction between the adsorbed molecules. Furthermore, relatively high values of n were reflected in the fact that the adsorption of Cu(II) and Pb(II) ions onto the geopolymer was highly favorable. Table 3 summarizes the adsorption capacities of different adsorbents toward Cu(II) and Pb(II) ions based on literature reports.

3.6. Adsorption mechanism

The geopolymer has many mesopores, thus it has a certain pore adsorption capacity, that is, physical adsorption, and this adsorption has no selectivity. However, according to EDS and kinetic results, the adsorption of Cu(II) and Pb(II) ions by geopolymer is chemisorption, which is dominated by ion exchange.

The heavy metal adsorption mechanism on the geopolymer is illustrated in Fig. 10. Metal ions (copper ions) are exchanged with sodium ions present in the structure of geopolymer and then sodium ions are released into the solution. The adsorption process of Cu(II) and Pb(II) ions is similar; therefore, only the behavior of adsorbed Cu(II) ions is shown in the figure. Besides, it can be considered that physisorption also exists at the same time during immobilization of heavy metals based on the BET analysis.

3. Conclusions

In the present study, the metakaolin-based geopolymer was utilized as an efficient adsorbent for the removal of Cu(II) and Pb(II) ions from the aqueous solution. In the batch test studies, the optimal adsorption conditions (pH, adsorption dose, contact time, initial metal ion concentration) for the effective adsorption of metal ions were investigated. SEM–EDS studies showed that the adsorption process was accompanied by ion exchange. The kinetic data fitted well with a pseudo-second-order kinetic model, indicating the existence of chemisorption between geopolymer and metal ions during adsorption process. The isotherm studies indicated that the adsorption of Cu(II) and Pb(II) ions followed the Langmuir adsorption isotherm model. The maximum adsorption capacity of Cu(II) (mmol/g) was higher than that of Pb(II). The geopolymer is an effective and inexpensive adsorbent, which can be efficiently used to remove heavy metal ions from aqueous solutions.

Acknowledgment

This work was supported by the Guangdong Science and Technology Department (2014A020209077, 2017A030223007, 2017GKZDXM007).

References

[1] K. Yin, Q. Wang, M. Lv, L. Chen, Microorganism remediation strategies towards heavy metals, Chem. Eng. J., 360 (2019) 1553–1563.

[2] Q. Chen, Y. Yao, X. Li, J. Lu, J. Zhou, Z. Huang, Comparison of heavy metal removals from aqueous solutions by chemical precipitation and characteristics of precipitates, J. Water Process Eng., 26 (2018) 289–300.

[3] A. Giwa, A. Dindi, J. Kujawa, Membrane bioreactors and electrochemical processes for treatment of wastewaters containing heavy metal ions, organics, micropollutants and dyes: recent developments, J. Hazard. Mater, 370 (2019) 172–195.

[4] W. Cai, Z. Li, J. Wei, Y. Liu, Synthesis of peanut shell based magnetic activated carbon with excellent adsorption performance towards electroplating wastewater, Chem. Eng. Res. Des., 140 (2018) 23–32.

[5] R. Supitcha, Rapid Preparation of biosorbents with high ion exchange capacity from rice straw and bagasse for removal of heavy metals, Sci. World J., 2014 (2014) 1–9.

[6] S.W. Ali, F. Waqar, M.A. Malik, T. Yasin, B. Muhammad, Study on the synthesis of a macroporous ethylacrylate-divinylbenzene copolymer, its conversion into a bi-functional cation exchange resin and applications for extraction of toxic heavy metals from wastewater, J. Appl. Polym. Sci., 129 (2013) 2234–2243.

[7] J.-L. Han, X. Xia, M.R. Haider, W.-L. Jiang, Y. Tao, M.-J. Liu, H.-C. Wang, Y.-C. Ding, Y.-N. Hou, H.-Y. Cheng, Functional graphene oxide membrane preparation for organics/inorganic salts mixture separation aiming at advanced treatment of refractory wastewater, Sci. Total Environ., 628 (2018) 261–270.

[8] M. Kraus, U. Trommler, F. Holzer, F.-D. Kopinke, U. Roland, Competing adsorption of toluene and water on various zeolites, Chem. Eng. J., 351 (2018) 356–363.

[9] P. Ding, W. Song, Z. Yang, J. Jian, Influence of Zn (II) stress-induction on component variation and sorption performance of extracellular polymeric substances (EPS) from Bacillus vallismortis, Bioprocess. Biosyst. Eng., 41 (2018) 781–791.

[10] J. Davidovits, Geopolymers: Ceramic-Like Inorganic Polymers, Geopolymer Institute, Saint-Quentin, France, 2017, pp. 335–350.

[11] P. Duan, C. Yan, W. Zhou, D. Ren, Development of fly ash and iron ore tailing based porous geopolymer for removal of Cu (II) from wastewater, Ceram. Int., 42 (2016) 13507–13518.

[12] İ. Kara, D. Yilmazer, S.T. Akar, Metakaolin based geopolymer as an effective adsorbent for adsorption of zinc (II) and nickel (II) ions from aqueous solutions, Appl. Clay Sci., 139 (2017) 54–63.

[13] C. Heah, H. Kamarudin, A.M. Al Bakri, M. Bnhussain, M. Luqman, I.K. Nizar, C. Ruzaidi, Y. Liew, Study on solids-to-liquid and alkaline activator ratios on kaolin-based geopolymers, Constr. Build. Mater., 35 (2012) 912–922.

[14] M. Alshaaer, Two-phase geopolymerization of kaolinite-based geopolymers, Appl. Clay Sci., 86 (2013) 162–168.

[15] H. Liu, S. Peng, L. Shu, T. Chen, T. Bao, R.L. Frost, Effect of Fe_3O_4 addition on removal of ammonium by zeolite NaA, J. Colloid Interface Sci., 390 (2013) 204–210.
[16] Y. Ge, X. Cui, Y. Kong, Z. Li, Y. He, Q. Zhou, Porous geopolymeric spheres for removal of Cu (II) from aqueous solution: synthesis and evaluation, J. Hazard. Mater, 283 (2015) 244–251.
[17] C. Sarkar, J.K. Basu, A.N. Samanta, Removal of Ni^{2+} ion from waste water by Geopolymeric Adsorbent derived from LD Slag, J. Water Process Eng., 17 (2017) 237–244.
[18] M. Catauro, F. Bollino, F. Papale, G. Lamanna, Investigation of the sample preparation and curing treatment effects on mechanical properties and bioactivity of silica rich metakaolin geopolymer, Mater. Sci. Eng., C, 36 (2014) 20–24.
[19] X. Guo, H. Shi, Self-solidification/stabilization of heavy metal wastes of class C fly ash–based geopolymers, J. Mater. Civ. Eng., 25 (2012) 491–496.
[20] F.J. López, S. Sugita, M. Tagaya, T. Kobayashi, Metakaolin-based geopolymers for targeted adsorbents to heavy metal ion separation, J. Mater. Sci. Chem. Eng., 2 (2014) 16.
[21] T. Cheng, M. Lee, M. Ko, T. Ueng, S. Yang, The heavy metal adsorption characteristics on metakaolin-based geopolymer, Appl. Clay Sci., 56 (2012) 90–96.
[22] I. Kara, D. Tunc, F. Sayin, S.T. Akar, Study on the performance of metakaolin based geopolymer for Mn (II) and Co (II) removal, Appl. Clay Sci., 161 (2018) 184–193.
[23] P. Hadi, J. Barford, G. McKay, Toxic Heavy metal capture using a novel electronic waste-based material mechanism, modeling and comparison, Environ. Sci. Technol., 47 (2013) 8248–8255.
[24] L. Mihaly-Cozmuta, A. Mihaly-Cozmuta, A. Peter, C. Nicula, H. Tutu, D. Silipas, E. Indrea, Adsorption of heavy metal cations by Na-clinoptilolite: equilibrium and selectivity studies, J. Environ. Manage, 137 (2014) 69–80.
[25] S. Lagergren, Zur theorie der sogenannten adsorption geloster stoffe, Kungliga svenska vetenskapsakademiens. Handlingar, 24 (1898) 1–39.
[26] H. Liu, C. Wang, J. Liu, B. Wang, H. Sun, Competitive adsorption of Cd(II), Zn(II) and Ni(II) from their binary and ternary acidic systems using tourmaline, J. Environ. Manage, 128 (2013) 727–734.
[27] I. Langmuir, The adsorption of gases on plane surfaces of glass, mica and platinum, J. Am. Chem. Soc., 40 (1918) 1361–1403.
[28] M. Kapur, M.K. Mondal, Competitive sorption of Cu (II) and Ni (II) ions from aqueous solutions: kinetics, thermodynamics and desorption studies, J. Taiwan Inst. Chem. Eng., 45 (2014) 1803–1813.
[29] M.-q. Jiang, Q.-p. Wang, X.-y. Jin, Z.-l. Chen, Removal of Pb (II) from aqueous solution using modified and unmodified kaolinite clay, J. Hazard. Mater., 170 (2009) 332–339.
[30] J. He, Y. Li, C. Wang, K. Zhang, D. Lin, L. Kong, J. Liu, Rapid adsorption of Pb, Cu and Cd from aqueous solutions by β-cyclodextrin polymers, Appl. Surf. Sci., 426 (2017) 29–39.
[31] S. Andrejkovičová, A. Sudagar, J. Rocha, C. Patinha, W. Hajjaji, E.F. da Silva, A. Velosa, F. Rocha, The effect of natural zeolite on microstructure, mechanical and heavy metals adsorption properties of metakaolin based geopolymers, Appl. Clay Sci., 126 (2016) 141–152.
[32] H.R. Khalid, N. Lee, S. Park, N. Abbas, H. Lee, Synthesis of geopolymer-supported zeolites via robust one-step method and their adsorption potential, J. Hazard. Mater., 353 (2018) 522–533.
[33] Y. Liu, P. Qian, Y. Yu, B. Yu, Y. Wang, S. Ye, Y. Chen, Preparation and characterization of a novel hybrid chelating material for effective adsorption of Cu (II) and Pb (II), J. Environ. Sci., 67 (2018) 224–236.
[34] Q. Xu, Y. Wang, L. Jin, Y. Wang, M. Qin, Adsorption of Cu (II), Pb (II) and Cr (VI) from aqueous solutions using black wattle tannin-immobilized nanocellulose, J. Hazard. Mater., 339 (2017) 91–99.
[35] M.A. Khaleque, Large-pore diameter nano-adsorbent and its application for rapid lead(II) detection and removal from aqueous media, Chem. Eng. J., 273 (2015) 286–295.
[36] M. Ghasemi, M. Naushad, N. Ghasemi, Y. Khosravi-Fard, A novel agricultural waste based adsorbent for the removal of Pb(II) from aqueous solution: Kinetics, equilibrium and thermodynamic studies, J. Ind. Eng. Chem., 20 (2014) 454–461.
[37] M.R. Awual, G.E. Eldesoky, T. Yaita, M. Naushad, H. Shiwaku, Z.A. Alothman, S. Suzuki, Schiff based ligand containing nano-composite adsorbent for optical copper(II) ions removal from aqueous solutions, Chem. Eng. J., 279 (2015) 639–647.
[38] M. Naushad, Z.A. Alothman, M.M. Alam, M.R. Awual, G.E. Eldesoky, M. Islam, Synthesis of sodium dodecyl sulfate-supported nanocomposite cation exchanger: removal and recovery of Cu^{2+} from synthetic, pharmaceutical and alloy samples, J. Iran. Chem. Soc., 12 (2015) 1–10.
[39] Mu. Naushad, A.Z. Alothman, M. Rabiul Awual, M. Mezbaul Alam, E.G. Eldesoky, Adsorption kinetics, isotherms, and thermodynamic studies for the adsorption of Pb^{2+} and Hg^{2+} metal ions from aqueous medium using Ti(IV) iodovanadate cation exchanger, Ionics (Kiel), 21 (2015) 2237–2245.